

Geodetic Determination of Relative Plate Motion in Central California

J. C. SAVAGE AND R. O. BURFORD

*National Center for Earthquake Research
U.S. Geological Survey, Menlo Park, California 94025*

Geodetic data along the San Andreas fault between Parkfield and San Francisco, California (latitudes 36°N and 38°N, respectively), have been re-examined to estimate the current relative movement between the American and Pacific plates across the San Andreas fault system. The average relative right lateral motion is estimated to be 32 ± 5 mm/yr for the period 1907–1971. Between 36°N and 37°N it appears that most, if not all, of the plate motion is accommodated by fault creep. Although strain is presumably accumulating north of 37°N (San Francisco Bay area), the geodetic evidence for accumulation is not conclusive.

We have re-examined the geodetic data pertinent to the determination of the relative motion between the Pacific and American plates along the 280-km-long segment of the San Andreas fault that extends southeast from San Francisco (Figure 1). The data consist of repeated surveys of triangulation networks over the period 1907–1962, repeated surveys over the period 1960–1970 of the geodimeter network shown in Figure 1, and direct measurements of fault creep mostly in the period 1968–1971. The objective is to determine the relative motion of geodetic stations (e.g., Santa Ana and Mt. Toro in Figure 1) on opposite sides of, and at some distance from, the faults in the San Andreas system.

Figure 2 shows two simple models of plate motion along a transform fault. The plates slip past one another in response to shear stresses that presumably originate from the drag of mantle convection currents upon the bottom of the lithosphere plates. Our present understanding of the San Andreas fault system suggests that below about 15-km depth the plates slip past one another fairly uniformly along a steep contact; i.e., a condition of continuous stable sliding may very well prevail at depth, as is evidenced by rather uniform long-term displacement rates measured at the surface and by an apparent absence of earthquake foci at depths greater than about 15 km. Along certain segments of the fault (e.g., Parkfield to Hollister; see Figure 1) continuous or quasi-continuous

slip (called fault creep) occurs at the surface; this behavior presumably represents an extension of the area of stable sliding on the fault surface upward through the entire crust, so that the motion measured across the segment over a few years is similar to the motion in the rigid-block model shown in the lower part of Figure 2. In other regions (e.g., the section of the San Andreas fault from just north of Hollister to well north of San Francisco) the upper portion of the fault surface appears to be locked, and strain should accumulate in the vicinity of the fault (upper sketches in Figure 2). In measuring relative motion of the plates across a section where the fault is locked, it is of course necessary to be sure that the measurements extend far enough beyond the fault to span the zone of strain accumulation. This distance turns out to be surprisingly large. A rough estimate of it can be obtained from a dislocation model similar to that shown in the upper part of Figure 2. For simplicity we assume that slip on the fault is zero down to depth D but is an amount b everywhere below that depth. Then, in the coordinate system shown in Figure 2, the strike slip displacement v and the tensor shear strain e_{xy} on the free surface are given from the simple screw dislocation model [Weertman and Weertman, 1964] by

$$\begin{aligned} v &= (b/\pi) \arctan(x/D) \\ e_{xy} &= (bD/2\pi)(x^2 + D^2)^{-1} \end{aligned} \quad (1)$$

Both quantities are plotted as functions of x/D on the right-hand side of Figure 2. Most of the

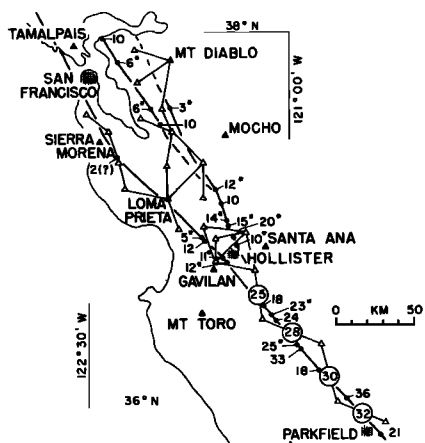


Fig. 1. The San Andreas fault system between Parkfield and San Francisco. The principal faults, shown by heavy sinuous lines, are, from west to east, the San Andreas, Hayward, and Calaveras. The solid triangles represent stations in the primary triangulation scheme. The lines connecting triangles show the California geodimeter network. (The four lines farthest south are identified by numbers 25, 28, 30, 32. The other lines are identified in Figure 7.) Observations of fault creep (in millimeters per year) are shown by numbers along the faults. Fault creep data marked by * are from Nason [1971]; other data are from R. O. Burford (unpublished data, 1971).

15 km, as is commonly accepted, measurements must extend to 100 km on either side of the fault. It is this requirement that creates the principal obstacle to interpreting geodetic data on plate movement: any result can be challenged on the basis that measurements may not have extended sufficiently far from the fault. On the other hand, where the rigid-block type of motion obtains, there is no particular difficulty in measuring relative block motion.

TRIANGULATION DATA

Part of the primary scheme of triangulation in California spans the San Andreas fault system. Repeated surveys of this system by the U.S. Coast and Geodetic Survey have furnished invaluable data on relative movement across the fault system. Whitten [1948] compared the geodetic positions of the stations shown in Figure 3 as determined from the surveys of 1906, 1922, and 1946 to determine the relative movement of the stations. The geodetic positions were calculated subject to the assumption that the position and length of the line Mocho-Mt. Diablo was the same for each survey. The results of Whitten's analysis are shown by arrows originating at each station in Figure 3. It appears that Santa Ana and Tamalpais have undergone no significant net displacement in the period 1906-1946, whereas Mt. Toro, Gavilan, Loma Prieta, and Sierra Morena have all moved northwest approximately parallel to the fault at average rates of 49, 48, 32, and 36

relative movement is concentrated close to the fault (e.g., 50% of the relative motion occurs between $x = -D$ and $x = +D$, but, to include 90% of the relative motion, measurements must be made across a zone extending from $x = -6.3D$ to $x = +6.3D$. Thus if D is about

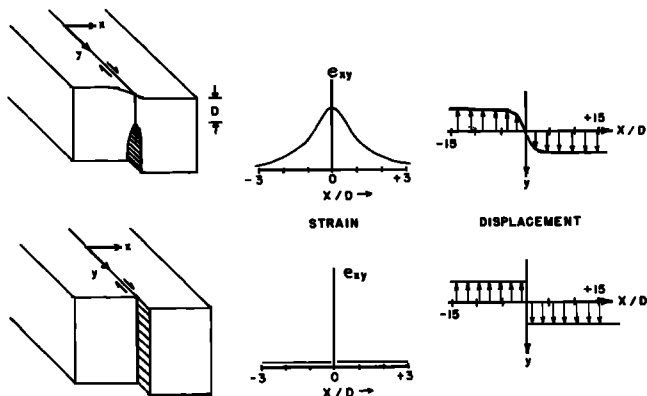


Fig. 2. Simple models for fault motion showing the distribution of shear strain and strike slip displacement on the surface. The upper sketches refer to a locked-fault model, in which slip on the fault occurs only at depths greater than D . The lower sketches refer to the rigid-block model, in which slip is approximately uniform with depth.

mm/yr, respectively. Because these results are contaminated by appreciable errors accumulated in carrying the triangulation network forward from the base Mocho-Mt. Diablo, it is probable that the 17-mm/yr difference between the lowest and highest rates is not significant. The magnitudes of the accumulated errors are suggested by the apparent movement at Santa Ana (1 meter northwest in 1906–1922 and 1 meter southeast in 1922–1946). Presumably Santa Ana remained fixed relative to Mocho-Mt. Diablo during the entire period (all three stations are on the same plate well back from the fault), and the apparent motions in 1906–1922 and 1922–1946 merely represent accumulated survey error. Thus corrections of similar magnitude and direction (i.e., 1 meter southeast for 1906–1922 and 1 meter northwest for 1922–1946) should be applied to the displacements at Mt. Toro and Gavilan. Such corrections would clearly make the motions at these stations more uniform for the two periods of time. The point we wish to make here is that significant errors accumulate in triangulation adjustments, but the relative motion of nearby stations is preserved.

The relative motion between nearby stations can frequently be calculated directly from the observed changes in azimuth. For example, in cases where the azimuth between two stations is approximately perpendicular to a fault, the component parallel to the fault of the displacement between those two stations is simply the product of the azimuth change and the distance between stations. Such a calculation would apply, for example, to the line Santa Ana-Mt. Toro in Figure 3. Alternatively, if one assumes that the relative motion is parallel to the fault strike, the magnitude of the displacement can readily be calculated from changes in azimuth even though that azimuth is not even approximately perpendicular to the fault strike. *Whitten* [1948] and *Meade* [1963] have applied these techniques to the triangulation network in Figure 3. We have used their data for surveys in 1882, 1906, 1922, 1947, 1951, 1957, and 1962 to show in Figure 4 the calculated relative displacement as a function of time. For the lines approximately perpendicular to the fault strike (Mt. Diablo-Sierra Morena, Mocho-Loma Prieta, Santa Ana-Mt. Toro, and Santa Ana-Gavilan) the method gives the component of displacement

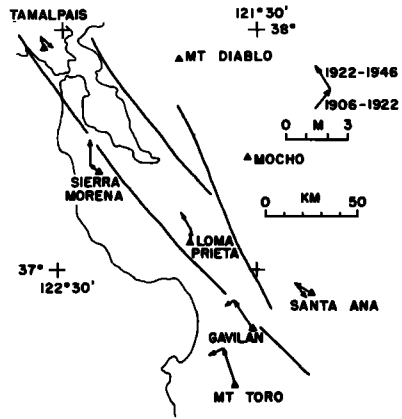


Fig. 3. Movement of stations in the primary scheme of triangulation from a comparison of the adjusted surveys of 1906, 1922, and 1946 [after *Whitten*, 1948]. The arrows represent the apparent station displacement in the periods 1906–1922 and 1922–1946.

ment parallel to the strike of the San Andreas fault; for the other lines in Figure 4 we have assumed that the relative displacement is parallel to the fault. As can be seen, the data do define reasonably linear trends. The slopes of the trends have been calculated from a least-squares analysis of all data except the 1882 survey (the 1882 survey was excluded from the fit because the interval 1882–1906 would contain the sudden displacements associated with the San Francisco earthquake of 1906); the slopes, along with the standard deviation indicated by the least-squares analysis, are shown in Figure 4.

Although it does not form part of the primary triangulation network, Farallon L.H., a lighthouse on a small island about 36 km southwest of the San Andreas fault (Figure 5), has been intersected in surveys of 1855, 1882, 1906, 1922, 1948, and 1957. The accuracy of the azimuth to Farallon L.H. is, of course, somewhat lower than azimuths in the primary scheme. Nevertheless, the position of Farallon L.H. (so far seaward from the fault) makes it desirable to attempt to ascertain its motion from the observed changes in azimuth. Figure 5 shows the two lines to the Farallon L.H., one from Tamalpais and one from Sonoma Mountain, which have been used to calculate the right lateral relative motion of Farallon L.H. For the motion

of Farallon L.H. relative to Tamalpais we added the azimuth of Mt. Diablo from Tamalpais in the main-scheme triangulation to the observed (i.e., unadjusted) angle at Tamalpais from Mt. Diablo to Farallon L.H. to calculate the azimuth

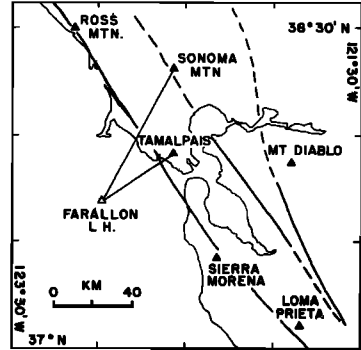


Fig. 5. Map showing the location of Farallon L.H. relative to the main scheme of triangulation. The faults (heavy lines) are, from left to right, the San Andreas fault, the Hayward-Rogers Creek-Healdsburg system, and the Calaveras-Green Valley system.

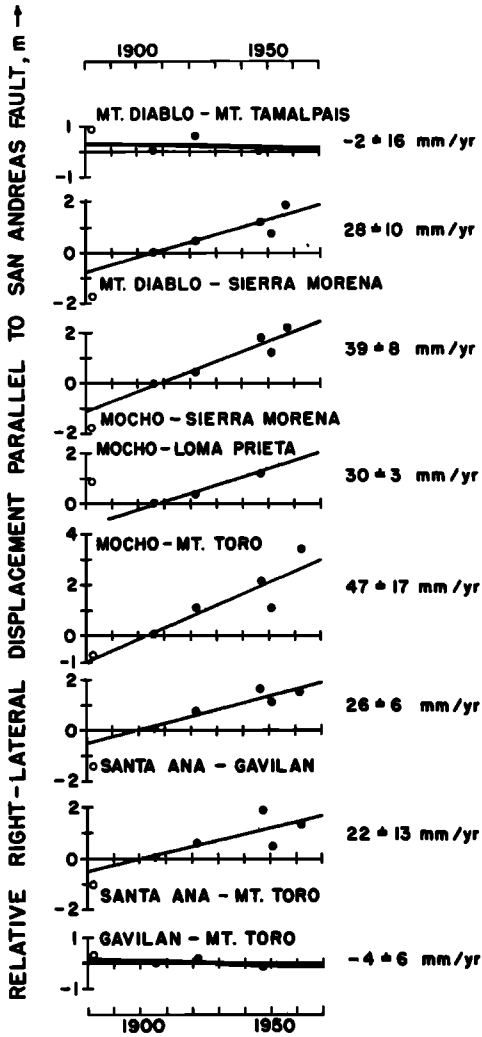


Fig. 4. Relative right lateral displacement as a function of time for stations in the primary triangulation scheme (Figure 3) as calculated from observed changes in azimuth [from *Whitten*, 1948; *Meade*, 1963]. The average rate of motion in millimeters per year as calculated by a least-squares linear fit to the postearthquake (1906) data is shown beside each plot. The uncertainty quoted is one standard deviation, as obtained from the least-squares analysis. The pre-1906 observations (open circles) were not included in the least-squares fit.

of Farallon L.H. The results (Figure 6) suggest a right lateral motion of 8 ± 1 mm/yr for Farallon L.H. relative to Tamalpais. That motion can also be calculated by using the angle from Farallon L.H. to Ross Mountain (see Figure 5) measured at Tamalpais. Because the line Tamalpais-Ross Mountain is parallel to the San Andreas fault, it is reasonable to assume that its azimuth remains fixed. Thus the change in azimuth of Farallon L.H. from Tamalpais should be equal to (but of opposite sign from) the change in the angle Farallon L.H. to Ross Mountain measured at Tamalpais. That analysis suggests a right lateral motion of Farallon L.H. relative to Tamalpais of 25 ± 11 mm/yr, an estimate that, because of its large standard deviation, does not differ significantly (i.e., within the 95% confidence level) from the earlier estimate of 8 ± 1 mm/yr. The second estimate (25 ± 11 mm/yr) does suggest very strongly, however, that the standard deviation (± 1 mm/yr) of the earlier estimate is much too low, a result that is not very surprising in view of the fact that the least-squares fit was based on only 3 data points.

The right lateral motion of Farallon L.H. relative to Sonoma Mountain (Figure 5) can be estimated from the change in the angle between Mt. Diablo and Farallon L.H. measured at Sonoma Mountain. Because the line Mt. Diablo-Sonoma Mountain is practically parallel to the San Andreas fault, its azimuth is not likely to change appreciably. Thus the change in the

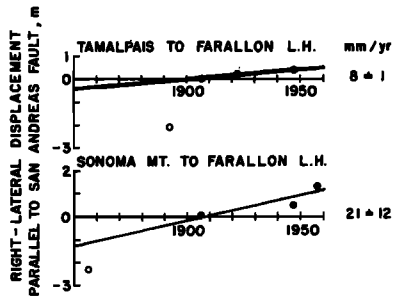


Fig. 6. Relative right lateral displacement as a function of time for Farallon L.H. relative to Tamalpais and Sonoma Mountain (Figure 5) as calculated from observed changes in azimuth. The average rate of motion in millimeters per year as calculated by a least-squares linear fit to the post-earthquake (1906) data is shown beside each plot. The uncertainty quoted is one standard deviation. The pre-earthquake data (open circles) were not included in the least-squares fit.

angle Mt. Diablo to Farallon L.H. at Sonoma Mountain is equal to the change in azimuth of Farallon L.H. to Sonoma Mountain. The changes in the azimuth so calculated suggest a right lateral motion of Farallon L.H. relative to Sonoma Mountain of 21 ± 12 mm/yr (Figure 6).

Dr. C. A. Whitten (quoted by Bolt [1970, p. 34]) has investigated the movement of Farallon L.H. relative to Mt. Diablo, Sonoma Mountain, and Ross Mountain as indicated by the surveys of 1882, 1906, 1922, 1948, and 1957. Whitten adjusted the results subject to the assumption that Mt. Diablo, Sonoma Mountain, and Ross Mountain all remained fixed, and he found that Farallon L.H. moved N 14° W at the rate of 46 mm/yr. The indicated motion is quite closely parallel to the strike of the San Andreas fault (N 35° W) in this area. Whitten's value should be compared with our own estimate of 21 ± 12 mm/yr for the right lateral motion of Farallon L.H. relative to Sonoma Mountain. The standard deviation of our own estimate (± 12 mm/yr) is sufficiently large that the estimate itself is probably not inconsistent with Whitten's value. However, we believe that Whitten's estimate is subject to very appreciable uncertainty. It is very doubtful that Ross Mountain, scarcely 6 km from the section of the San Andreas fault that underwent 3.5 meters of slip in 1906, has remained fixed relative to Sonoma Mountain

and Mt. Diablo, as is assumed in Whitten's adjustment. If it has not remained fixed, its movement would introduce a bias tending to cause the right lateral movement of Farallon L.H. to be overestimated. Thus there is reason to believe that Whitten's estimate may be too high.

A triangulation network (Salinas River valley net) extending northwest from Parkfield along the San Andreas fault to within about 30 km of Hollister was established in 1944 and resurveyed in 1963. The network covers a zone extending laterally from a few kilometers northeast of the San Andreas fault to about 40 km southwest of the fault. Meade and Small [1966] compared geodetic positions calculated from the two adjusted surveys to detect relative movement across the San Andreas fault. That comparison showed clearly that all the significant relative movement occurred within a few kilometers of the fault; there was no significant relative motion between stations on the same side of the fault (i.e., on the same fault block). The measurements are quite consistent with the rigid-block model shown in the lower half of Figure 2. Meade and Small [1966] also calculated the right lateral component of motion across the fault from the change in azimuth of six lines that crossed the fault approximately perpendicular to strike. They found the average rate of right lateral slip across the fault was 32 ± 1 mm/yr.

A triangulation network (the Monterey Bay arc) with a high density of stations was extended in 1930 from the coastline north of Mt. Toro to Santa Ana, crossing the San Andreas fault system near Hollister (see Figure 1 for locations). The network was resurveyed in 1951 and 1962. This network has been discussed by Whitten [1960] and by Savage and Burford [1970]. Savage and Burford compared the observed angles for the three surveys and concluded that within the accuracy of the surveys there was no evidence for strain accumulation in the blocks on either side of the fault system. The relative motion between blocks appeared to be accommodated by slip on San Andreas and Calaveras faults or strain accumulation in very narrow zones centered on those faults. Savage and Burford estimated the combined relative right lateral slip across the San Andreas and Calaveras faults to be 25 ± 1 mm/yr.

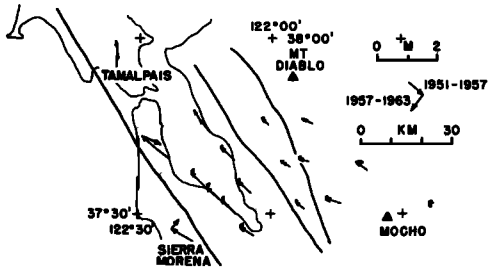


Fig. 7. Movement (indicated by arrows) of stations in the San Francisco Bay area from comparison of the adjusted triangulation surveys of 1951, 1957, and 1962. In the calculation the length and azimuth of the line Mt. Diablo-Mocho were assumed to remain invariant in the interval 1951-1962. The data are from *Pope et al.* [1966].

Excluding slip on the faults, they estimated the average right lateral strain accumulation across the 70-km-wide zone to be $0.04 \pm 0.08 \mu$ strain/yr which is equivalent to 3 ± 5 mm/yr right lateral relative motion of the end points of the arc. Thus, the analysis of *Savage and Burford* [1970] leads to an estimate of 28 ± 5 mm/yr right lateral motion for a point near Mt. Toro relative to a point near Santa Ana.

Finally, a high-density triangulation network was established in 1951 in the area between Mt. Diablo and Mocho on the east and Sierra Morena and Tamalpais on the west (Figure 7). This network was resurveyed in 1957 and 1962. *Pope et al.* [1966] have shown that the surveys suggest a large right lateral movement (80 cm for Sierra Morena relative to Mocho) distributed across the network during the period 1951-1957 but negligible and rather random motion in the period 1957-1962. These motions are indicated by arrows in Figure 7. As *Whitten* [1959] pointed out, a close examination of the displacement pattern for the period 1951-1957 suggests the possibility of a clockwise rotation of the whole network relative to the fixed base line Mt. Diablo-Mocho. Such an apparent rotation would result if the observation from either end of the base line to the other end were deflected by horizontal refraction. Dr. C. A. Whitten (verbal communication, 1971) has informed us that up to 4 seconds of horizontal refraction has recently been observed from Mocho, and it does seem possible that the 1951 survey might have been similarly affected. This possibility is supported by the observation that

all the 1951 data in Figure 4 are too low; in fact, the values are so low that they require left rather than right lateral motion across the San Andreas fault system in the period 1947-1951. An error in the 1951 azimuth of the line Mt. Diablo-Mocho would also explain this anomaly. Thus we feel that the large right lateral motions inferred from the 1951-1962 San Francisco Bay area triangulation data are probably the consequence of horizontal refraction in the base line observations of 1951. The alternative to this explanation is to accept a highly irregular relative movement between the Pacific and American plates (left lateral slip in 1947-1951, very rapid right lateral slip in 1951-1957, and no slip in 1957-1962). We believe that an error in the azimuth observations in 1951 is much more likely. An error of this magnitude can be tolerated in a long-term series of observations such as are shown in Figure 4; however, it will completely dominate the changes in a period as short as 1951-1957.

GEODIMETER DATA

Figure 1 shows the northern part of the California geodimeter network, which extends along the San Andreas fault. The network was established in 1959 and was surveyed approximately annually until 1968 by the California Division of Water Resources. Since 1968 it has been surveyed by the California Division of Mines and Geology. Line length measurements are available for a period of 9 to 12 years for each of the lines shown in Figure 1, and the data for most of these lines exhibit a trend in time. We have taken this trend as defined by a least-squares linear fit to represent the average rate of change of line length (dL/dt), and that value, along with its standard deviation, will be used in this analysis to estimate fault slip and strain accumulation.

The geodimeter network near Hollister contains a rigid configuration (Figure 8) that permits a unique solution (exclusive of displacements generated by rigid-body motions of the figure as a whole) for the relative motions of the five stations involved. *Savage and Burford* [1971] have already discussed this solution, and it will suffice here to review it briefly. We chose to calculate motions relative to Browns, and for the moment we neglect the effects of possible rigid rotations of the figure by requir-

ing that the azimuth of line 21 remain fixed. Then the observed rates of lengthening of the lines involved determine the relative motions of the stations as shown by the arrows in Figure 8. The restriction to a fixed azimuth for line 21 can be removed by adding any motion generated by a rigid rotation of the trilateration figure about Browns. Clearly such a rotation imposes a component of motion perpendicular to the fault system at Fairview as well as at other stations. Because the length of line 21 has not changed significantly ($dL/dt = 2 \pm 1$ mm/yr) and the line itself is practically parallel to the San Andreas fault, we do not think it likely that station Fairview has moved significantly with respect to Browns. Thus we doubt that any significant rotation should be imposed on the trilateration figure, and consequently we believe that the annual rate vectors shown in Figure 8 are approximately correct.

A similar solution of the trilateration network shown in Figure 8 can be obtained by making the plausible assumption that all motions are parallel to the San Andreas fault system. Then the changes in the lengths of the pairs of lines that link Fairview to Fremont dictate the relative right lateral motion between those points. Lines 17 and 23 require a relative motion of 32 ± 5 mm/yr, lines 18 and 22 require 27 ± 4 mm/yr, and lines 20 and 21 require 27 ± 3 mm/yr. (The same assumption requires that Sargent and Gilroy both move at the rate of 15 ± 4 mm/yr relative to Fairview.) Fault creep has been measured at several localities along the Calaveras and San Andreas faults near Hollister (see Figure 1). The average value for fault creep on the Calaveras in this sector is seen to be 15 ± 2 mm/yr and on the San Andreas 10 ± 2 mm/yr. Thus it would appear that all the relative movement detected by the geodimeter network can be accounted for by observed fault creep.

Next let us consider the geodimeter network north of Hollister (Figures 1 and 9). The geodimeter data for this area are generally less satisfactory than data found elsewhere, and we have chosen to show the individual length measurements as a function of time (Figure 10), so that the reader can judge for himself the uncertainties in the analysis. Before 1969 measurements were made with a Model 2A Geodimeter, and the correction of atmospheric refrac-

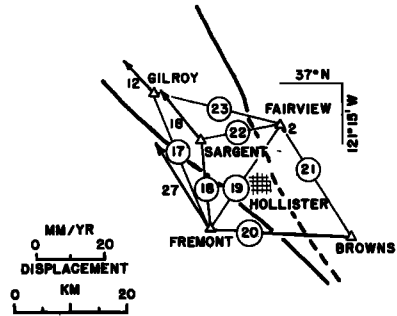


Fig. 8. Trilateration network near Hollister. The arrows represent the average rate of displacement of the stations relative to Browns for the period 1960–1970 as inferred from the average rate of lengthening of the observed lines.

tivity was based on measurements at the end points and occasionally on a balloon measurement at the midpoint [Hofmann, 1968]; later measurements (shown as solid points in the figure) were made with laser instruments (geodolite or Model 8 Geodimeter), and the correction for atmospheric refractivity was measured simultaneously from an aircraft flying along the line of sight. The later measurements are of course somewhat more accurate, but a careful examination of the data indicates no systematic error was introduced by changing the method of measurement. The linear least-squares fit to the data for each line is shown in Figure 10, and the slope of that line (dL/dt) along with its standard deviation is shown beside the line in Figure 9.

The configuration of the geodimeter net near Loma Prieta (Figure 11) is such that one can estimate the relative right lateral motion across the San Andreas fault system, which at that latitude consists of three strands (the Calaveras, the Hayward, and the San Andreas proper). Lines 6 and 13 in Figure 11 are nearly colinear and can be taken together to approximate a single long line from Loma Prieta to Allison. Then the triangle Loma Prieta-Allison-Mt. Hamilton forms a rigid configuration that can be analyzed for relative motions (again excluding possible motions generated by rigid rotations of the figure as a whole). We shall calculate the motions relative to Mt. Hamilton and, to eliminate the contributions from rigid rotation of the figure, hold the azimuth of line 7 fixed. Then the rates of lengthening of lines

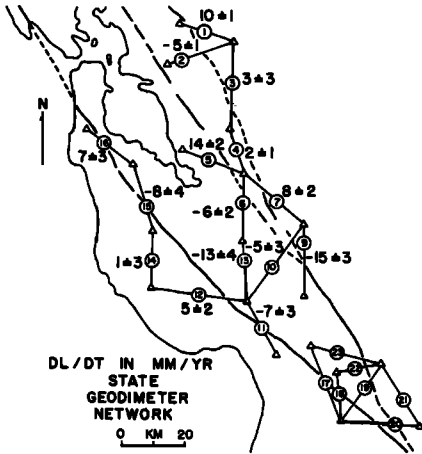


Fig. 9. Geodimeter network in the vicinity of San Francisco Bay. The numbers beside the lines represent the average rate of lengthening (with standard deviation) of the line in millimeters per year. The Hollister trilateration network (Figure 8) is shown in the lower right.

6, 7, 10, and 13 determine the motions of Allison and Loma Prieta, as is shown by the arrows in Figure 11. The restriction to a fixed azimuth for line 7 can be removed by adding any motions generated by a rigid-body rotation of the triangle Loma Prieta-Allison-Mt. Hamilton about Mt. Hamilton. Such rotations add a component of motion at Allison that is perpendicular to the trend of the San Andreas system. Inasmuch as the predominant motion at all stations should be at least approximately parallel to the San Andreas fault, the additional component at Allison produced by the acceptable rotations must be rather small. The rotational contribution at Loma Prieta must be of almost equal magnitude to that at Allison (lines 7 and 10 are of similar length) but will be almost parallel to the San Andreas fault (because line 10 is almost perpendicular to the fault). Thus we have established that Loma Prieta must move parallel to the fault trend at a rate of about 31 ± 6 mm/yr plus or minus a few millimeters per year associated with possible rigid-body rotations of the trilateration figure. The latter contribution is small compared with the uncertainty in the former estimate and can be neglected. We can proceed further by assuming that the other stations in Figure 11 also move parallel to the trend of the San Andreas fault. The observed values of dL/dt for the various lines (Figure 9) then re-

quire that the motions of the stations relative to Mt. Hamilton be as they are shown by the dashed arrows and numbers in Figure 11. The indicated relative right lateral motion across the fault system in this area appears to be 38 ± 7 mm/yr (Eagle Rock relative to Mt. Hamilton).

The configuration of the geodimeter network southeast of Hollister (lines 25, 28, 30, and 32 in Figure 1) does not permit a unique solution for the relative motion across the fault system. However, it appears reasonable to assume that the motions are approximately parallel to the fault trend, in which case it is easy to infer the amount of relative right lateral motion required between stations at the ends of each line. The values for the individual lines are shown in Table 1, and a mean value for the relative right lateral motion appears to be 32 ± 3 mm/yr for the decade 1960-1970. Fault creep has been measured at several localities along this section of the fault (Figure 1). The measurements generally refer to the right lateral motion observed across a zone about 100 meters wide centered on the active trace of the fault. The measurements in this section range from 18 to 36 mm/yr, with an average value of about 25 ± 6 mm/yr. There is reason to believe that such direct measurements of fault creep may underestimate the over-all relative motion within the fault zone [Savage and Burford, 1971], and for this reason the higher values may be more reliable; nevertheless, the average measured value for fault creep (25 ± 6 mm/yr) is not significantly different from the average inferred from geodimeter measurements (32 ± 3 mm/yr).

CONCLUSIONS

The measurements of relative motion across the San Andreas fault system between Parkfield and San Francisco are summarized in Table 2. For convenience that segment of the fault has been divided into three sections (northern, central, and southern), with the dividing points about 30 km northwest and 30 km southeast of Hollister. In quoting triangulation results from Figure 4 in Table 2, only lines approximately normal to the San Andreas fault system have been used, so as to obtain more reliable estimates of relative right lateral motion.

For the southern section the evidence is quite good that the measured value (32 mm/yr) does represent the total relative right lateral motion

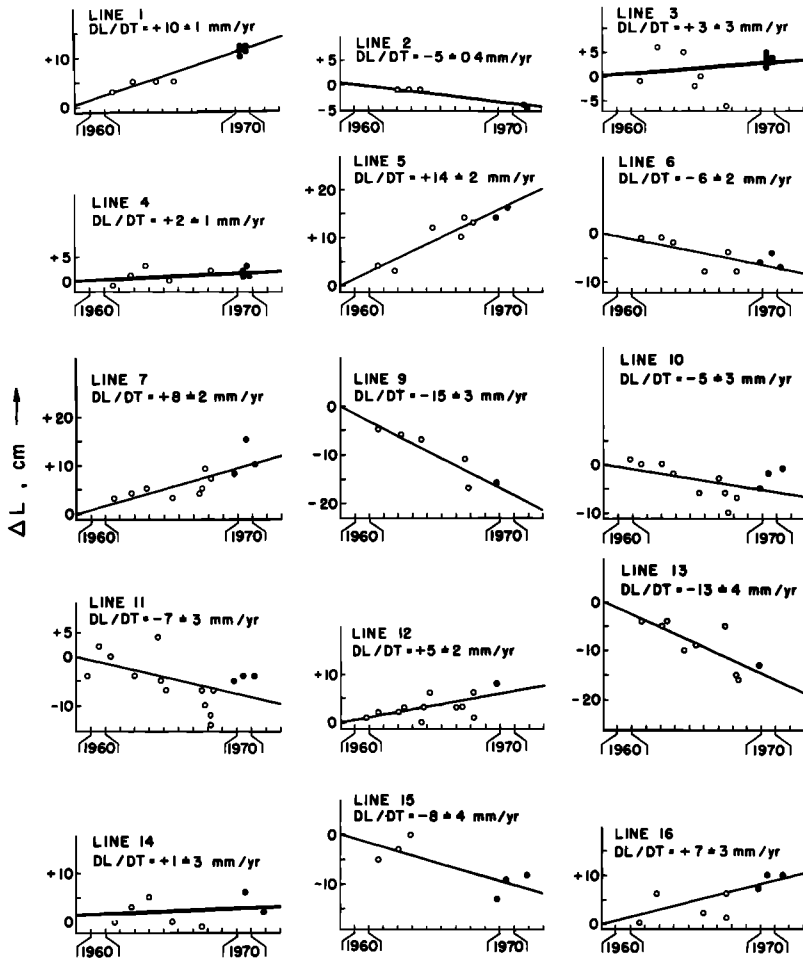


Fig. 10. Change of line length as a function of time for geodimeter lines in the San Francisco Bay area. The open data points represent measurements by the California Department of Water Resources, and the solid points represent more recent measurements, in which atmospheric refractivity was determined simultaneously from an aircraft. The straight line in each plot represents the least-squares linear fit to the data. The slope of that line is quoted with its standard deviation as the average rate of lengthening (dL/dt).

across the San Andreas fault system. The triangulation data for the Salinas River valley network, 1944–1963 [Meade and Small, 1966], show no evidence of relative motion within the block southwest of the fault (i.e., no measurable strain). Moreover, the relative right lateral motion measured by the geodimeter network is in reasonable agreement with fault creep measured within 100 meters of the active fault trace. Thus the evidence certainly suggests rigid-block motion of the type shown in the lower sketch of Figure 2. The evidence that all the

relative plate motion has been measured in the central section is also quite good. The primary scheme of triangulation (Figures 3 and 4) shows that Mt. Toro and Gavilan both move within the limits of significance at the same rate relative to Santa Ana, as we should expect for the rigid-block model. Similarly no significant movement between Mt. Toro and Gavilan (both on the same fault block) is demonstrated in Figure 4 (in fact, the indicated motion, though not significantly different from zero, is left lateral). However, because of the large

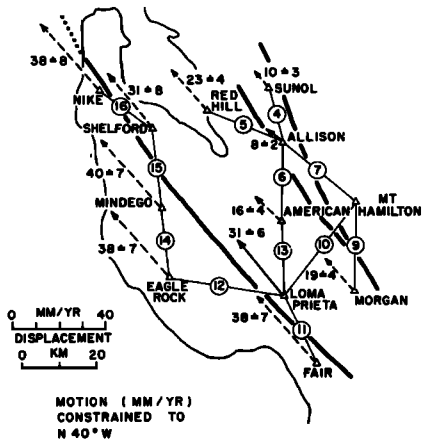


Fig. 11. Station displacement rates relative to Mt. Hamilton for stations in the Bay area geodimeter network as inferred from the rate of change of line lengths. In most cases the information was inadequate to determine the motion without imposing the constraint that it was parallel to the San Andreas fault (N 40°W); for those cases displacement rate is indicated by a dashed rather than solid arrow. The rates of displacement (with standard deviations) in millimeters per year are shown beside the arrows.

standard deviations these data do not exclude the possibility of some relative movement between stations on the same fault block (e.g., within the 95% confidence level Mt. Toro could move northwest at the rate of 8 mm/yr relative to Gavilan). Similarly the analysis of *Savage and Burford* [1970] demonstrated no significant relative motion in the fault blocks on either side of the fault system, but they could not exclude such movement below the level of significance in their analysis (about 7 mm/yr across 70 km at the 95% confidence level). The most convincing evidence that the rigid-block model applies is the fact that

TABLE 1. Rate of Change of Line Length and Indicated Right Lateral Motion for Geodimeter Lines South of Hollister

Line	Period for which Data Are Available	dL/dt , mm/yr	Relative Right Lateral Motion, mm/yr
25	1959 to 1971	28 ± 1	35 ± 2
28	1959 to 1971	25 ± 2	28 ± 2
30	1960 to 1971	28 ± 3	29 ± 3
32	1959 to 1971	35 ± 3	37 ± 3

observed fault creep on the Calaveras (about 14 mm/yr) and the San Andreas (about 12 mm/yr) faults is adequate to explain the observed plate motion, as was discussed previously [Savage and Burford, 1971]. Finally, the various estimates of relative block movement for the central section in Table 2 are quite consistent despite the fact that they refer to measurements that span zones of different width across the fault system. In the analysis of the northern section (Table 2), there is somewhat greater uncertainty that the geodetic control does extend far enough either to the east or to the west to be sure that all the relative movement between plates has been included. The excellent agreement between the movement of Loma Prieta relative to Mocho (30 ± 3 mm/yr from Figure 4) and relative to Mt. Hamilton (31 ± 6 mm/yr from Figure 11) suggests the absence of significant relative motion between Mocho and Mt. Hamilton. The fact that all the stations on the block southwest of the San Andreas fault in Figure 11 move at the same velocity relative to Mt. Hamilton suggests that none of the relative motion extends appreciably west of the San Andreas fault. However, the standard deviations associated with both observations are large enough that we cannot exclude relative motion

TABLE 2. Summary of Relative Motions of Blocks on Opposite Sides of the San Andreas Fault System between Parkfield and San Francisco

Section of Fault	Triangulation Data, mm/yr	Geodimeter Data, 1960 to 1970 mm/yr
Southern	32 ± 1*	32 ± 3
Central	26 ± 6† 22 ± 13‡ 28 ± 5	28 ± 4
Northern	28 ± 10¶ 39 ± 8** 21 ± 12††	38 ± 7

*Salinas River Valley network, 1944 to 1963 [Meade and Small, 1966].

†Santa Ana-Gavilan, 1906 to 1962, Figure 4.

‡Santa Ana-Mt. Toro, 1906 to 1962, Figure 4.

||Monterey Bay arc, 1930 to 1962 [Savage and Burford, 1970].

¶Mt. Diablo-Sierra Morena, 1906 to 1957, Figure 4.

**Mocho-Sierra Morena, 1906 to 1957, Figure 4.

††Sonoma Mountain-Farallon L.H., 1906 to 1957, Figure 6.

within the block east of the Calaveras fault or west of the San Andreas fault. Perhaps more direct evidence on the lack of relative movement within the western block is the absence of a significant change in length for geodimeter line 14 (Figure 9), which lies wholly within that block. Less definite evidence for the lack of relative movement within the eastern blocks is afforded by the absence of significant change in length of line 4 (Figure 9). The primary triangulation data for the northern section in Table 2 extend only to Sierra Morena, which lies only about 3 km southwest of the San Andreas fault. The station apparently was displaced 1.7 meters to the northwest relative to Mocho-Mt. Diablo at the time of the 1906 San Francisco earthquake [Hayford and Baldwin, 1908]. This of course indicates that the same amount of relative right lateral motion must have accumulated to the west of the station in an unknown interval of time preceding the earthquake of 1906. Thus the primary triangulation data for the northern section in Table 2 may underestimate the relative plate motion by an amount of the order of 17 mm/yr (based on the 100-year recurrence interval between great earthquakes). On the other hand, absence of any significant shortening in geodimeter line 14 indicates that relative right lateral motion is not accumulating west of Sierra Morena at present, and the supplemental triangulation data (last entry in Table 2), which extend far seaward to Farallon L.H., suggest an even lower rate of relative motion across the San Andreas system than do the primary triangulation data.

Examination of Table 2 shows that, within the limits of error in measurement, all the estimates are consistent with a relative right lateral motion of about 32 mm/yr across the San Andreas fault system. This agreement obtains despite the fact that in the southern section all the accommodation appears to be concentrated within 1 km of the fault trace, in the central section it appears to be concentrated on two faults (San Andreas and Calaveras) about 20 km apart, and in the northern section it appears to be spread over more than 40 km. It is true that the agreement would be more impressive if the standard deviations of the individual measurement were somewhat smaller; nevertheless, the remarkable coincidence of so many different measurements is compelling evidence for ac-

cepting a rate near 32 mm/yr. Moreover, the fault movement in the southern and central sections seems to be predominantly, if not entirely, of the rigid-block type (lower sketch in Figure 2). Thus the problem of whether geodetic measurements extend sufficiently far from the fault to include all significant movement is not involved. After examining all the uncertainties we have rather subjectively assigned a standard deviation of ± 5 mm/yr to the estimated relative plate motion, so that the final value we propose is 32 ± 5 mm/yr.

The motion of Tamalpais at the extreme north end of the network may be anomalous. The arrows in Figure 3 certainly suggest no net movement of Tamalpais with respect to Mt. Diablo and Mocho. However, when the repeated observations are plotted as a function of time (Figure 4) the uncertainty of the relative motion (-2 ± 16 mm/yr) is clearly demonstrated; indeed, the data in that figure indicate that within the 95% confidence limits the motion could be identical with that at Loma Prieta (30 mm/yr right lateral), a station that occupies a comparable position relative to the fault system.

There does appear to be a pattern of motion across both the San Andreas fault and the Calaveras-Hayward fault system in Figure 11. A right lateral motion of about 19 ± 2 mm/yr across the Calaveras-Hayward system is suggested by the indicated movements of Red Hill, American, and Morgan relative to Mt. Hamilton. Similarly a right lateral motion of about 7 ± 2 mm/yr across the San Andreas fault is suggested by the indicated movements of Nike, Mindego, and Eagle Rock relative to Loma Prieta and Shelford. The motion of the stations on the southwest side of the Calaveras-Hayward system (i.e., the line of stations Red Hill, American, and Morgan) relative to those on the northeast side of the San Andreas fault (i.e., stations Loma Prieta and Shelford) can be estimated only from the data for the single connecting geodimeter line, line 13. The indicated relative right lateral motion is 16 ± 5 mm/yr, a rate that is surprisingly large in view of the fact that line 13 does not cross one of the recognized throughgoing faults. It is unfortunate that no other suitably oriented geodimeter line crosses the gap from the southwest side of the Calaveras-Hayward fault system to the northeast side of the San Andreas fault; it would be

of great interest to have an independent check on the results indicated by line 13.

The data in Figure 6 on the motion of Farallon L.H. are roughly consistent with the picture outlined above. The relative right lateral movement of 8 ± 1 mm/yr from Tamalpais to Farallon L.H. is quite consistent with the observed 7-mm/yr movement across the San Andreas fault. The right lateral movement (21 ± 12 mm/yr) of Farallon L.H. relative to Sonoma Mountain is reasonably well within the expected range for a relative movement across the San Andreas fault system of 32 ± 5 mm/yr. A value somewhat lower than 32 mm/yr might be expected for the line Sonoma Mountain to Farallon L.H. because it may not span the complete zone of the San Andreas fault system (Figure 5). Thus the data for the northern tier of stations (Mt. Diablo, Tamalpais, Sonoma Mountain, and Farallon L.H.) are consistent with our over-all interpretation.

The sites of fault creep observations in the fault system in central California are shown in Figure 1. Within the area shown in Figure 11, fault creep has been observed on the Calaveras and Hayward faults but not on the San Andreas fault. (An offset of about 6 mm in an alignment array established in 1968 on the San Andreas fault near the crossing with geodimeter line 15, shown in Figure 9, has been observed, but it is not clear that this motion is a real measure of fault creep. It is shown in Figure 1 as questionable.) The observations illustrated in Figure 1 suggest that about 10 mm/yr of fault creep occurs along the Hayward-Calaveras fault system in the area where lines 6, 7, 9, and 10 cross the system. The pattern of fault creep suggests that slip is transferred from the Calaveras to the Hayward near the point where the latter branches off from the former (i.e., just south of the crossing with line 9). Because the transfer of slip is not a simple process, we are not at all sure that the measurements of fault creep reported here represent all the deformation within the fault zone. We suspect there may be concentrated deformation within the thin wedge that separates the Calaveras and Hayward faults in this area. However, the measured values (10 mm/yr) for fault creep in this area are somewhat less than the displacement across the Hayward-Calaveras system inferred from geodimeter measurements (19 ± 2 mm/yr).

The data for lines 1, 2, and 3 (Figure 9) do not appear to be consistent with any simple interpretation. The change in line 1 certainly suggests right lateral motion across the Calaveras fault, but the change in line 3 is inconsistent with such motion. Line 2 appears to be shortening at the rate of 5 mm/yr, whereas simple right lateral motion models would suggest that it should be extending at a very low rate. Perhaps an argument could be advanced for omitting line 3 because of the scatter in line length measurements shown in Figure 8. (However, we find it hard to see how the trend could be reversed to a negative slope even by rejecting data.) But even if line 3 is omitted, it is difficult to explain the seemingly inconsistent behavior of lines 1 and 2.

The geodimeter data in Figure 9 do not really fit either of the models of Figure 2. The rigid-block model (lower sketch in Figure 2) does not apply because the measured fault creep appears inadequate to explain the observed motion and also because line 13 has lengthened significantly even though it does not cross a recognized throughgoing fault. The locked-fault model (upper sketch in Figure 2) apparently does not apply because lines 3, 4, and 14 would be expected to shorten appreciably, whereas they actually lengthen, although by an insignificant amount. It is not completely clear that the discrepancies are wholly due to the inadequacies of the models; it is possible that the difficulty is due to extraneous trends in the data (e.g., incomplete observation of fault creep, station instability leading to erroneous values of dL/dT , or apparent trends in Figure 10 introduced by random error). We think some of the difficulty in interpreting the data may be associated with the branching of the Hayward fault from the Calaveras fault in the vicinity of lines 9 and 10. It is likely that strain may be distributed in a somewhat unusual manner at such a *Y* junction.

It is perhaps worth showing that the geodimeter data in the San Francisco Bay area do not fit a pattern of uniform strain accumulation. Figure 12 shows the average strain rate ($L^{-1} dL/dt$) as a function of azimuth for each of the geodimeter lines. The continuous curve represents the uniform strain rate field, determined by least squares, that best fits the observed data. The principal strain rates for the

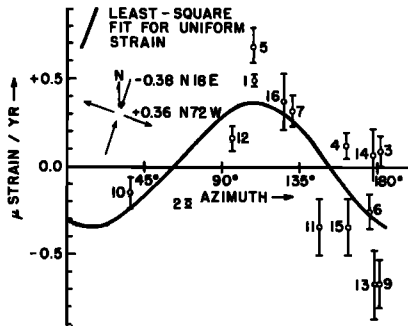


Fig. 12. Average strain rates for lines in the Bay area geodimeter network as a function of azimuth (measured clockwise from north). The points are identified by line number, and the error bars represent one standard deviation on either side of the point. If the strain field in the Bay area were uniform, a sinusoidal curve would fit the points. The best uniform field fit as determined by least squares is shown by the heavy line, and the principal axes of the best-fit strain field are shown as an inset in the figure.

field are also shown in the figure. It is clear that the field is not a reasonable fit to the observations.

Meade [1971] has discussed measurements from 1906 (postearthquake) to 1969 on a small triangulation figure (8-km aperture) that spans the San Andreas fault near Ross Mountain (Figure 5). The data indicate approximately uniform right lateral shear strain accumulation at the rate of $0.55 \pm 0.05 \mu$ strain/yr. (The value quoted is for the tensor shear, not the engineering shear, as used by Meade; the former is half of the latter.) There was no indication of fault creep along the trace of the 1906 rupture, which passes through the triangulation figure. The locked-fault model (upper sketch Figure 2) is presumed to apply to the San Andreas fault in this region, and we can use equation 1 to obtain an estimate of the depth D below which slip occurs. Using our estimate of relative plate motion ($b = 32$ mm/yr) and Meade's measurement (0.55μ strain/yr) for the peak strain (i.e., $x = 0$ in equation 1), we find $D = 9$ km. Because the simple screw dislocation model (no slip above depth D and constant slip below) is grossly oversimplified, the value of D quoted must be understood as representing some intermediate depth within the zone of transition from complete slip to no slip.

Chinnery [1961] has used the values, mea-

sured near Ross Mountain, of the surface deformation associated with the San Francisco earthquake of 1906 to calculate the depth to which sudden slip extended at the time of the earthquake. He used a screw dislocation model that is just the complement of the one used in (1): constant slip to a depth D and no slip beneath that depth. From the observed deformation Chinnery estimated D to be not more than 6 km and perhaps as small as 2 km. Again, because of the oversimplified model, this depth estimate must be understood as representing some intermediate depth within the zone of transition from complete slip to no slip. Presumably the region that slips during the earthquake is the region that did not slip continuously before the earthquake. Thus we would expect that Chinnery's estimate of D (2–6 km) should be approximately the same as our own estimate (9 km); this of course assumes that the region of fault creep does not progressively approach closer to the surface until failure occurs. Chinnery's comparatively low value of D would indicate a proportionately lower value of b (e.g., 16 mm/yr); such a low value would suggest that part of the relative plate motion is being carried by the northern continuations of the Hayward and Calaveras faults (Rodgers Creek-Healdsburg faults and Green Valley fault, respectively). However, in view of the tremendous oversimplifications involved in the screw dislocation models, it is possible that the difference between the two estimates of D is not significant.

Acknowledgments. The 1968 geodimeter data in Figure 10 were furnished through the courtesy of the California Division of Mines and Geology; the data for 1969–1971 were furnished through a cooperative effort of the California Division of Mines and Geology, the U.S. Geological Survey, and the University of California, Berkeley (through NSF grant GA 12205 to B. A. Bolt and F. H. Moffitt). All the triangulation measurements were made by the U.S. Coast and Geodetic Survey (now National Geodetic Survey).

Publication has been authorized by the Director, U.S. Geological Survey.

REFERENCES

- Bolt, B. A., Cause of earthquakes, in *Earthquake Engineering*, edited by R. L. Wiegel, pp. 21–45, Prentice Hall, Englewood Cliffs, N. J., 1970.
Chinnery, M. A., Deformation of the ground

- around surface faults, *Bull. Seismol. Soc. Amer.*, 51, 355-372, 1961.
- Hofmann, R. B., Geodimeter fault movement investigations in California, *Calif. Dep. Water Resour. Bull.*, no. 116, part 6, 183 pp., 1968.
- Hayford, J. F., and A. L. Baldwin, Geodetic measurements of earth movements, in *The California Earthquake of April 18, 1906*, vol. 1, pp. 114-145, Carnegie Institution of Washington, D. C., 1908.
- Meade, B. K., Horizontal crustal movements in the United States, 25 pp., *U.S. Coast Geod. Surv.*, Washington, D. C., 1963.
- Meade, B. K., Horizontal movement along the San Andreas fault system, *Roy. Soc. N. Z. Bull.*, 9, 175-179, 1971.
- Meade, B. K., and J. B. Small, Current and recent movement on the San Andreas fault, *Calif. Div. Mines Geol. Bull.*, 190, 385-391, 1966.
- Nason, R. D., Investigations of fault creep slippage in Northern and Central California, Ph.D. thesis, 231 pp., Univ. of Calif., San Diego, 1971.
- Pope, A. J., J. L. Stearns, and C. A. Whitten, Surveys for crustal movement along the Hayward fault, *Bull. Seismol. Soc. Amer.* 56, 317-323, 1966.
- Savage, J. C., and R. O. Burford, Strain accumulation in California, *Bull. Seismol. Soc. Amer.*, 60, 1877-1896, 1970.
- Savage, J. C., and R. O. Burford, Discussion of paper by C. H. Scholz and T. J. Fitch, 'Strain accumulation along the San Andreas fault,' *J. Geophys. Res.*, 76, 6469-6479, 1971.
- Weertman, J., and J. R. Weertman, *Elementary Dislocation Theory*, 213 pp., Macmillan, New York, 1964.
- Whitten, C. A., Horizontal earth movement, vicinity of San Francisco, California, *Eos Trans. AGU*, 29, 318-323, 1948.
- Whitten, C. A., Notes on remeasurement of triangulation net in the vicinity of San Francisco, Calif., *Calif. Div. Mines Geol. Spec. Rep.* 57, 56-57, 1959.
- Whitten, C. A., Horizontal movement in the earth's crust, *J. Geophys. Res.*, 65, 2839-2844, 1960.

(Received May 23, 1972;
revised October 4, 1972.)